ASTROBIOLOGY
Volume 2, Number 1, 2002
© Mary Ann Liebert, Inc.

Research Paper

Mass-Independent Fractionation of Sulfur Isotopes in Archean Sediments: Strong Evidence for an Anoxic Archean Atmosphere

A.A. PAVLOV[1] and J.F. KASTING[2]

ABSTRACT

Mass-independent fractionation (MIF) of sulfur isotopes has been reported in sediments of Archean and Early Proterozoic Age (>2.3 Ga) but not in younger rocks. The only fractionation mechanism that is consistent with the data on all four sulfur isotopes involves atmospheric photochemical reactions such as SO_2 photolysis. We have used a one-dimensional photochemical model to investigate how the isotopic fractionation produced during SO_2 photolysis would have been transferred to other gaseous and particulate sulfur-bearing species in both low-O_2 and high-O_2 atmospheres. We show that in atmospheres with O_2 concentrations $<10^{-5}$ times the present atmospheric level (PAL), sulfur would have been removed from the atmosphere in a variety of different oxidation states, each of which would have had its own distinct isotopic signature. By contrast, in atmospheres with O_2 concentrations $\geq 10^{-5}$ PAL, all sulfur-bearing species would have passed through the oceanic sulfate reservoir before being incorporated into sediments, so any signature of MIF would have been lost. We conclude that the atmospheric O_2 concentration must have been $<10^{-5}$ PAL prior to 2.3 Ga.
Key Words: Anoxic Archean atmosphere—Mass-independent fractionation—Atmospheric sulfur cycle. Astrobiology 2, 27–41.

INTRODUCTION

THE QUESTION of how much O_2 was present in the Archean atmosphere has been debated for a long time. Although most researchers agree that the level of atmospheric oxygen was substantially lower prior to 2.0–2.3 Ga (Cloud, 1972; Walker, 1977; Walker *et al.*, 1983; Kasting, 1993; Holland, 1994), some scientists have continued to argue that the atmosphere was oxygen-rich throughout the Archean (Towe, 1994; Ohmoto, 1996, 1997). Holland (1994) summarized a variety of forms of geological evidence that favor reduced oxygen levels prior to ~2.2 Ga: the absence of red beds, the presence of banded iron formations (until 1.8 Ga), the lack of oxidation of Fe^{2+} in paleosols, and the widespread presence of detrital uraninite and pyrite in sediments. However, each of these arguments allows for alternative interpretations (Ohmoto, 1996, 1997). Nevertheless, based on paleosol and uranium data, Holland (1994) estimated that O_2 concentrations were $<10^{-2}$ times the present atmospheric level (PAL) prior to 2.2 Ga. Other authors using photochemical models predict much lower

---

[1] Laboratory for Atmospheric and Space Physics, University of Colorado, Boulder, CO.
[2] Department of Geosciences, The Pennsylvania State University, University Park, PA.

ground-level O_2 concentrations ($\sim 10^{-12}$–10^{-8} PAL) in the Archean–Early Proterozoic atmosphere (Kasting, 1993; Pavlov *et al.*, 2001).

Complicating the picture even more is the discovery of molecular fossils of biological lipids (Brocks *et al.*, 1999; Summons *et al.*, 1999), which indicates that both cyanobacteria and eukaryotes were present by 2.7 Ga. This suggests that oxygen should have been present in at least some areas of the surface ocean. Although this does not necessarily imply oxygen in the atmosphere (Kasting, 1992), some researchers have continued to insist that atmospheric O_2 must therefore have been abundant.

Recently, however, Farquhar *et al.* (2000a) presented evidence for sulfur isotope mass-independent fractionation (MIF) in sediments deposited prior to ~2.3 Ga. These data have since been verified by two independent investigations (Mojzsis *et al.*, 2001; G. Hu and D. Rumble, personal communication). Most thermodynamic, kinetic, or biological processes in aqueous solution or solid-phase fractionate isotopes in a mass-dependent way (i.e., mass-dependent relationship for sulfur isotopes: $\delta^{33}S \cong 0.515\delta^{34}S$; $\delta^{36}S \cong 1.91\delta^{34}S$). Note that the term "MIF" is somewhat misleading because fractionation does depend on the mass of the isotopes. MIF simply means that sulfur isotopes do not obey the standard mass-dependent relationship described above.

The only process known to produce MIF in solid or liquid phases results from hyperfine interactions (i.e., spin–orbit coupling in isotopes with odd-mass nuclei such as ^{33}S and ^{17}O). Farquhar *et al.* (2000a) ruled out this process as a possible explanation for the Archean sulfur isotope data because of the positive correlation between $\Delta^{33}S$ and $\Delta^{36}S$ (the deviations from the normal mass-dependent relationship). If MIF had originated from hyperfine interactions, $\Delta^{36}S$ should have been 0.

MIF in gas-phase reactions has been reported for a number of different photochemical processes (Thiemens, 1999; Zmolek *et al.*, 1999; Farquhar *et al.*, 2000b). Farquhar *et al.* (2001) showed experimentally that photolysis of SO_2 by UV radiation in the 190–220 nm spectral region produces MIF. The penetration of such short-wave radiation deep into the atmosphere could only have happened if the column abundances of ozone and oxygen were smaller than today. Farquhar *et al.* (2001) concluded that the Archean oxygen level must have been at least one to two orders of magnitude lower than at present, though they stopped short of estimating an actual upper limit on the concentration of O_2. A quantitative upper limit can only be obtained from model calculations such as those described here.

We argue that the sulfur isotopic data provide an even stronger constraint on atmospheric O_2 than suggested above. MIF of sulfur isotopes could only have occurred under reduced atmospheric conditions when sulfur was being removed from the atmosphere in a variety of different oxidation states (Kasting *et al.*, 1989). Therefore, the data of Farquhar *et al.* (2001) provide strong evidence for an almost completely anoxic Archean atmosphere.

MODEL DESCRIPTION

We have examined this problem using two different photochemical models of Earth's evolving atmosphere. The first, from Pavlov *et al.* (2001), represents a weakly reduced (CH_4/N_2-rich, O_2-poor), hypothetical Late Archean atmosphere. The second, adapted from Kasting *et al.* (1985), represents the atmosphere following the oxic transition at 2.3 Ga. O_2 concentrations in this atmosphere are allowed to vary between 10^{-5} and 1 PAL. Separate photochemical models are needed because some short-lived species become long-lived at higher O_2 levels, and vice versa. Numerical problems arise if one attempts to use the same model in both atmospheric regimens.

The one-dimensional photochemical model used in our Archean numerical experiments includes 72 "major" (excluding minor sulfur isotopes) chemical species involved in 337 reactions. The model is fully described in Pavlov *et al.* (2001). A list of all the chemical reactions that involve sulfur-bearing species is provided in Table 1.

In order to study isotopic fractionation, we added a subroutine to the model in which the sulfur photochemistry is duplicated for an isotopic species. For example, the reaction

$$S + HS \rightarrow S_2 + H$$

is replaced by two reactions for the isotopic species, S* (^{33}S, ^{34}S, ^{36}S):

$$S^* + HS \rightarrow S^*S + H$$

$$S + HS^* \rightarrow S^*S + H$$

Table 2 displays a list of the corresponding chemical reactions for sulfur isotopes. In compiling this list, we have made several assumptions:

1. We have assumed that chemical species containing minor sulfur isotopes (^{33}S, ^{34}S, ^{36}S) do not affect the concentration of major atmospheric species containing ^{32}S. This allows us to decouple the sulfur isotopic species from the rest of the model.
2. We have assumed that no chemical species can contain more than one atom of a minor sulfur isotope. In other words, we excluded species like S^*_2, SS^*_2, etc. This is acceptable because the most abundant minor sulfur isotope, ^{34}S, is still only 4.4% of the abundance of ^{32}S.
3. We also assumed that the probability of reaction between two minor sulfur isotopic species is negligible (i.e., we ignored reactions like $S^*O + S^*O \rightarrow S^*O_2 + S^*$).
4. In all our calculations we assumed that the only isotopic fractionation of any sort happens during the UV-photolysis of SO_2 (MIF). Subsequent atmospheric reactions do not produce additional MIF or mass-dependent fractionation. While this is not strictly true, we are interested here only in deviations from the normal terrestrial mass fractionation line. Thus, it is preferable to ignore all mass-dependent fractionation processes.

Our numerical procedure starts by dividing the atmosphere from 0 to 100 km into 1-km increments. At each height, the continuity equation was solved for each long-lived species, including transport by both eddy and molecular diffusion. The combined second-order partial differential equations were then cast in centered finite-difference form, and the resulting set of coupled ordinary differential equations was integrated to steady state using the reverse Euler method. After ~500 time steps (~10^8 model years), when all the "major" atmospheric species were converged, a similar numerical procedure was repeated for the minor sulfur isotopic species. During this second step, the concentrations of the "major" atmospheric species were treated as constants.

In our model the following species were considered long-lived (transport by diffusion included in the continuity equation): H_2S^*, HS^*, S^*, S^*O, S^*O_2, $H_2S^*O_4$, HS^*O, and S^*S. Four species, HS^*O_3, S^*O_3, S^*S_2, and S^*S_3, were assumed to be in equilibrium at each height step.

To test our model for physical consistency, we performed the following experiment: We assumed that SO_2 and S^*O_2 were outgassed at the same rate and there was no fractionation during SO_2 photolysis. If our model was coded correctly, chemical species like H_2S^*, HS^*, S^*, etc., would show no fractionation after the code was converged (i.e., $[H_2S^*] = [H_2S]$, etc.), and minor isotopic species containing multiple (n) sulfur atoms (e.g., S^*S and S^*S_3) should be n times as abundant as their major isotopic counterparts. Thus, $[S^*S] = 2[S_2]$, $[S^*S_3] = 4[S_4]$. The reason why this must be true is illustrated in Fig. 1.

Suppose, for simplicity, that the only source of sulfur is from volcanic outgassing of S and S* and that the only sulfur removal process is rainout of S_2 and S^*S. Let k and k' be the rates of chemical reactions of $S + S \rightarrow S_2$ and $S + S^* \rightarrow S^*S$, respectively. To conserve the number of sulfur atoms in steady state, the following should be true: $F_{in}(S) = 2F_{out}(S_2)$, and $F_{in}(S^*) = F_{out}(S^*S)$. If we assume that $F_{in}(S) = F_{in}(S^*)$, then the mixing ratio of S^*S must be twice that of S_2, while the mixing ratio of S* should be exactly equal to that of S. Both conditions can be satisfied only if $k' = 2k$ (i.e., reaction R*75 in Table 2).

Another type of adjustment of the chemical rate constants is more intuitive. Consider the reaction $S_2 + O \rightarrow S + SO$, with the rate constant k. For the isotopic molecule S^*S this reaction would split into two reactions: $S^*S + O \rightarrow S^* + SO$ and $S^*S + O \rightarrow S + S^*O$, each with rate constant k'. To maintain mass balance, we must have $k' = 0.5k$ (i.e., reactions R*73 and R*74 in Table 2).

These general rules of rate constant adjustment for the isotopic reactions can be stated as follows:

1. Double the rate constant when an isotopic species reacts with its "major" isotopic twin ($S + S^* \rightarrow S^*S$).
2. Halve the rates in reactions that branch in two directions ($S^*S + O \rightarrow S^* + SO$; $S^*S + O \rightarrow S + S^*O$).
3. Otherwise, the rates stay the same ($S^*O + O3 \rightarrow S^*O_2 + O_2$).

Our model, coded according to these rules, produced physically consistent results (i.e., when zero fractionation was assumed during SO_2 photodissociation, no fractionation was observed in any other sulfur-bearing atmospheric species).

For our higher-O_2 numerical simulations we used a one-dimensional photochemical model adapted from Kasting *et al.* (1985). The following improvements were made:

1. We calculated the UV flux for each layer using the same δ2-stream scattering approximation (Toon *et al.*, 1989) used in the Archean code (Pavlov *et al.*, 2001).

TABLE 1. SULFUR REACTIONS AND RATE CONSTANTS IN THE ARCHEAN ATMOSPHERE

	Reaction	*Rate constant* ($cm^3\ s^{-1}$)	*References*	*Notes*
Photolysis				
R1	$SO_2 + h\nu \rightarrow SO + O$	$1.34 \times 10^{-4}\ s^{-1}$	Warneck *et al.* (1964); Okabe (1971)	
R2	$SO_2 + h\nu \rightarrow S + O_2$			
R3	$SO_2 + h\nu \rightarrow {}^1SO_2$	$1.59 \times 10^{-3}\ s^{-1}$	Warneck *et al.* (1964); Okabe (1971)	
R4	$SO_2 + h\nu \rightarrow {}^3SO_2$	$8.69 \times 10^{-7}\ s^{-1}$	Warneck *et al.* (1964); Okabe (1971)	
R5	$H_2S + h\nu \rightarrow HS + H$	$2.20 \times 10^{-4}\ s^{-1}$	Sullivan and Holland (1966)	
R6	$H_2SO_4 + h\nu \rightarrow SO_2 + 2OH$	$8.74 \times 10^{-7}\ s^{-1}$	Turco *et al.* (1979)	a
R7	$HSO + h\nu \rightarrow HS + O$	$5.46 \times 10^{-4}\ s^{-1}\ (=J_{HO2})$	DeMore *et al.* (1985)	b
R8	$S_2 + h\nu \rightarrow S + S$	$9.74 \times 10^{-4}\ s^{-1}$	DeAlmeida and Singh (1986)	
R9	$S_3 + h\nu \rightarrow S_2 + S$	$(=J_{S2})$	See R8	b
R10	$S_4 + h\nu \rightarrow S_2 + S_2$	$(=J_{S2})$	See R8	b
Sulfur chemistry				
R11	${}^1SO_2 + M \rightarrow {}^3SO_2 + M$	1×10^{-12}	Turco *et al.* (1982)	
R12	${}^1SO_2 + M \rightarrow SO_2 + M$	1×10^{-11}	Turco *et al.* (1982)	
R13	${}^1SO_2 \rightarrow {}^3SO_2 + h\nu$	$1.5 \times 10^{3}\ s^{-1}$	Turco *et al.* (1982)	
R14	${}^1SO_2 \rightarrow SO_2 + h\nu$	$2.2 \times 10^{4}\ s^{-1}$	Turco *et al.* (1982)	
R15	${}^1SO_2 + O_2 \rightarrow SO_3 + O$	1×10^{-16}	Turco *et al.* (1982)	
R16	${}^1SO_2 + SO_2 \rightarrow SO_3 + SO$	4×10^{-12}	Turco *et al.* (1982)	
R17	${}^3SO_2 + M \rightarrow SO_2 + M$	1.5×10^{-13}	Turco *et al.* (1982)	
R18	${}^3SO_2 \rightarrow SO_2 + h\nu$	$1.13 \times 10^{3}\ s^{-1}$	Turco *et al.* (1982)	
R19	${}^3SO_2 + SO_2 \rightarrow SO_3 + SO$	7×10^{-14}	Turco *et al.* (1982)	
R20	$SO_2 + OH + M \rightarrow HSO_3 + M$	$k_0 = 3.0 \times 10^{-31}\ (300/T)^{3.3}$ $k_\infty = 1.5 \times 10^{-12}$	DeMore *et al.* (1992)	c
R21	$SO_2 + O + M \rightarrow SO_3 + M$	$3.4 \times 10^{-32} \exp(-1{,}130/T)[M]$	Turco *et al.* (1982)	
R22	$SO + O_2 \rightarrow O + SO_2$	$2.6 \times 10^{-13} \exp(-2{,}400/T)$	DeMore *et al.* (1992)	
R23	$SO + HO_2 \rightarrow SO_2 + OH$	2.8×10^{-11}	DeMore *et al.* (1992)	d
R24	$SO + O + M \rightarrow SO_2 + M$	$6.0 \times 10^{-31}\ [M]$	Kasting (1990)	b
R25	$SO + OH \rightarrow SO_2 + H$	8.6×10^{-11}	DeMore *et al.* (1992)	
R26	$SO + NO_2 \rightarrow SO_2 + NO$	1.4×10^{-11}	DeMore *et al.* (1992)	
R27	$SO + O_3 \rightarrow SO_2 + O_2$	$3.6 \times 10^{-12} \exp(-1{,}100/T)$	DeMore *et al.* (1992)	
R28	$SO + SO \rightarrow SO_2 + S$	8.3×10^{-15}	Herron and Huie (1980)	
R29	$SO + SO_3 \rightarrow 2SO_2$	2×10^{-15}	Yung and DeMore (1982)	
R30	$SO + HCO \rightarrow HSO + CO$	$5.5 \times 10^{-11}\ T^{0.4}$	Kasting (1990)	b
R31	$H + SO + M \rightarrow HSO + M$	$k_0 = 5.7 \times 10^{-32}\ (300/T)^{1.6}$ $k_\infty = 7.5 \times 10^{-11}$	Kasting (1990)	b
R32	$HSO_3 + O_2 \rightarrow HO_2 + SO_3$	$1.3 \times 10^{-12} \exp(-330/T)$	DeMore *et al.* (1992)	
R33	$HSO_3 + OH \rightarrow H_2O + SO_3$	1×10^{-11}	Kasting (1990)	b
R34	$HSO_3 + H \rightarrow H_2 + SO_3$	1×10^{-11}	Kasting (1990)	b
R35	$HSO_3 + O \rightarrow OH + SO_3$	1×10^{-11}	Kasting (1990)	b
R36	$SO_3 + H_2O \rightarrow H_2SO_4$	6.0×10^{-15}	DeMore *et al.* (1992)	
R37	$H_2S + OH \rightarrow H_2O + HS$	$6 \times 10^{-12} \exp(-75/T)$	DeMore *et al.* (1992)	
R38	$H_2S + H \rightarrow H_2 + HS$	$1.3 \times 10^{-11} \exp(-860/T)$	Baulch *et al.* (1976)	

R39	$H_2S + O \rightarrow OH + HS$	$9.2 \times 10^{-12} \exp(-1{,}800/T)$	DeMore *et al.* (1992)	
R40	$HS + O \rightarrow H + SO$	1.6×10^{-10}	DeMore *et al.* (1992)	
R41	$HS + O_2 \rightarrow OH + SO$	4.0×10^{-19}	DeMore *et al.* (1992)	
R42	$HS + HO_2 \rightarrow H_2S + O_2$	3×10^{-11}	McElroy *et al.* (1980)	
R43	$HS + HS \rightarrow H_2S + S$	1.2×10^{-11}	Baulch *et al.* (1976)	
R44	$HS + HCO \rightarrow H_2S + CO$	5×10^{-11}	Kasting (1990)	b
R45	$HS + H \rightarrow H_2 + S$	1.0×10^{-11}	Langford and Oldershaw (1972)	
R46	$HS + S \rightarrow H + S_2$	$2.2 \times 10^{-11} \exp(120/T)$	Kasting (1990)	b
R47	$HS + O_3 \rightarrow HSO + O_2$	$9.0 \times 10^{-12} \exp(-280/T)$	DeMore *et al.* (1992)	
R48	$HS + NO_2 \rightarrow HSO + NO$	$2.9 \times 10^{-11} \exp(240/T)$	DeMore *et al.* (1992)	
R49	$HS + H_2CO \rightarrow H_2S + HCO$	$1.7 \times 10^{-11} \exp(-800/T)$	DeMore *et al.* (1992)	
R50	$S + O_2 \rightarrow SO + O$	2.3×10^{-12}	DeMore *et al.* (1992)	
R51	$S + OH \rightarrow SO + H$	6.6×10^{-11}	DeMore *et al.* (1992)	
R52	$S + HCO \rightarrow HS + CO$	5×10^{-11}	Kasting (1990)	b
R53	$S + HO_2 \rightarrow HS + O_2$	1.5×10^{-11}	Kasting (1990)	b
R54	$S + HO_2 \rightarrow SO + OH$	1.5×10^{-11}	Kasting (1990)	b
R55	$S + O_3 \rightarrow SO + O_2$	1.2×10^{-11}	DeMore *et al.* (1992)	
R56	$S + CO_2 \rightarrow SO + CO$	1×10^{-20}	Yung and DeMore (1982)	b
R57	$S + S + M \rightarrow S_2 + M$	$2.76 \times 10^{-34} \exp(710/T)[M]$	Kasting (1990)	b
R58	$S + S_2 + M \rightarrow S_3 + M$	$2.8 \times 10^{-34}[M]$	Kasting (1990)	b
R59	$S + S_3 + M \rightarrow S_4 + M$	$(=k_{61})$	Kasting (1990)	b
R60	$S_2 + O \rightarrow S + SO$	1.1×10^{-11}	Hills *et al.* (1987)	
R61	$S_2 + S_2 + M \rightarrow S_4 + M$	$2.8 \times 10^{-31}[M]$	Baulch *et al.* (1976)	e
R62	$S_4 + S_4 + M \rightarrow S_8(AER) + M$	$(=k_{61})$	Kasting (1990)	b
R63	$HSO + NO \rightarrow HNO + SO$	$3.7 \times 10^{-12} \exp(250/T)$	Kasting (1990)	b
R64	$HSO + OH \rightarrow H_2O + SO$	$4.8 \times 10^{-11} \exp(250/T)$	Kasting (1990)	b
R65	$HSO + H \rightarrow HS + OH$	$8.1 \times 10^{-11} \times (0.90)$	Kasting (1990)	b
R66	$HSO + H \rightarrow H_2 + SO$	$8.1 \times 10^{-11} \times (0.08)$	Kasting (1990)	b
R67	$HSO + HS \rightarrow H_2S + SO$	1×10^{-12}	Kasting (1990)	b
R68	$HSO + O \rightarrow OH + SO$	$3.0 \times 10^{-11} \exp(200/T)$	Kasting (1990)	b
R69	$HSO + S \rightarrow HS + SO$	1×10^{-11}	Kasting (1990)	b

[a] Assumed equal to J_{HCl}.

[b] Estimated.

[c] Three-body rate constant given by:

$$k(M, T) = \left[\frac{k_0(T) \times [M]}{1 + \frac{k_0(T) \times [M]}{k_\infty(T)}} \right] \times 0.6^{\left\{1 + \left[\log \frac{k_0(T) \times [M]}{k_\infty(T)}\right]^2\right\}^{-1}}$$

[d] Assumed equal to rate for reaction of SO with ClO.

[e] No recommendation given; value based on measurement by Langford and Oldershaw (1972).

TABLE 2. SULFUR ISOTOPE REACTIONS AND RATE CONSTANTS IN THE ARCHEAN ATMOSPHERE

	Isotope reaction	*Corresponding major isotope reaction*	*Ratio of rate constants* k′/k
Photolysis			
R*1	$S^*O_2 + h\nu \rightarrow S^*O + O$	$SO_2 + h\nu \rightarrow SO + O$	1
R*2	$S^*O_2 + h\nu \rightarrow S^* + O_2$	$SO_2 + h\nu \rightarrow S + O_2$	1
R*3	$S^*O_2 + h\nu \rightarrow {}^1S^*O_2$	$SO_2 + h\nu \rightarrow {}^1SO_2$	1
R*4	$S^*O_2 + h\nu \rightarrow {}^3S^*O_2$	$SO_2 + h\nu \rightarrow {}^3SO_2$	1
R*5	$H_2S^* + h\nu \rightarrow HS^* + H$	$H_2S + h\nu \rightarrow HS + H$	1
R*6	$H_2S^*O_4 + h\nu \rightarrow S^*O_2 + 2OH$	$H_2SO_4 + h\nu \rightarrow SO_2 + 2OH$	1
R*7	$HS^*O + h\nu \rightarrow HS^* + O$	$HSO + h\nu \rightarrow HS + O$	1
R*8	$S^*S + h\nu \rightarrow S^* + S$	$S_2 + h\nu \rightarrow S + S$	1
R*9	$S^*S_2 + h\nu \rightarrow S^*S + S$	$S_3 + h\nu \rightarrow S_2 + S$	2/3
R*10	$S^*S_2 + h\nu \rightarrow S_2 + S^*$	$S_3 + h\nu \rightarrow S_2 + S$	1/3
R*11	$S^*S_3 + h\nu \rightarrow S^*S + S_2$	$S_2 + h\nu \rightarrow S_2 + S_2$	1
Sulfur chemistry			
R*12	${}^1S^*O_2 + M \rightarrow {}^3S^*O_2 + M$	${}^1SO_2 + M \rightarrow {}^3SO_2 + M$	1
R*13	${}^1S^*O_2 + M \rightarrow S^*O_2 + M$	${}^1SO_2 + M \rightarrow SO_2 + M$	1
R*14	${}^1S^*O_2 \rightarrow {}^3S^*O_2 + h\nu$	${}^1SO_2 \rightarrow {}^3SO_2 + h\nu$	1
R*15	${}^1S^*O_2 \rightarrow S^*O_2 + h\nu$	${}^1SO_2 \rightarrow SO_2 + h\nu$	1
R*16	${}^1S^*O_2 + O_2 \rightarrow S^*O_3 + O$	${}^1SO_2 + O_2 \rightarrow SO_3 + O$	1
R*17	${}^1S^*O_2 + SO_2 \rightarrow S^*O_3 + SO$	${}^1SO_2 + SO_2 \rightarrow SO_3 + SO$	0.5
R*18	${}^1S^*O_2 \rightarrow SO_2 + SO_3 + S^*O$	${}^1SO_2 \rightarrow SO_2 \rightarrow SO_3 + SO$	0.5
R*19	${}^1S^*O_2 + S^*O_2 \rightarrow S^*O_3 + SO$	${}^1SO_2 + SO_2 \rightarrow SO_3 + SO$	0.5
R*20	${}^1S^*O_2 + S^*O_2 \rightarrow SO_3 + S^*O$	${}^1SO_2 + SO_2 \rightarrow SO_3 + SO$	0.5
R*21	${}^3S^*O_2 + M \rightarrow S^*O_2 + M$	${}^3SO_2 + M \rightarrow SO_2 + M$	1
R*22	${}^3S^*O_2 \rightarrow S^*O_2 + h\nu$	${}^3SO_2 + SO_2 + h\nu$	1
R*23	${}^3S^*O_2 + SO_2 \rightarrow S^*O_3 + SO$	${}^3SO_2 + SO_2 \rightarrow SO_3 + SO$	0.5
R*24	${}^3S^*O_2 + SO_2 \rightarrow SO_3 + S^*O$	${}^3SO_2 + SO_2 \rightarrow SO_3 + SO$	0.5
R*25	${}^3S^*O_2 + S^*O_2 \rightarrow S^*O_3 + SO$	${}^3SO_2 + SO_2 \rightarrow SO_3 + SO$	0.5
R*26	${}^3S^*O_2 + S^*O_2 \rightarrow SO_3 + S^*O$	${}^3SO_2 + SO_2 \rightarrow SO_3 + SO$	0.5
R*27	$S^*O_2 + OH + M \rightarrow HS^*O_3 + M$	$SO_2 + OH + M \rightarrow HSO_3 + M$	1
R*28	$S^*O_2 + O + M \rightarrow S^*O_3 + M$	$SO_2 + H + M \rightarrow SO_3 + M$	1
R*29	$S^*O + O_2 \rightarrow O + S^*O_2$	$SO + O_2 \rightarrow O + SO_2$	1
R*30	$S^*O + HO_2 \rightarrow S^*O_2 + OH$	$SO + HO_2 \rightarrow SO_2 + OH$	1
R*31	$S^*O + O + M \rightarrow S^*O_2 + M$	$SO + O + M \rightarrow SO_2 + M$	1
R*32	$S^*O + OH \rightarrow S^*O_2 + H$	$SO + OH \rightarrow SO_2 + H$	1
R*33	$S^*O + NO_2 \rightarrow S^*O_2 + NO$	$SO + NO_2 \rightarrow SO_2 + NO$	1
R*34	$S^*O + O_3 \rightarrow S^*O_2 + O_2$	$SO + O_3 \rightarrow SO_2 + O_2$	1
R*35	$S^*O + SO \rightarrow S^*O_2 + S$	$SO + SO \rightarrow SO_2 + S$	1
R*36	$S^*O + SO \rightarrow S^*O_2 + S^*$	$SO + SO \rightarrow SO_2 + S$	1
R*37	$S^*O + SO_3 \rightarrow 2S^*O_2$	$SO + SO_3 \rightarrow 2SO_2$	1
R*38	$SO + S^*O_3 \rightarrow 2S^*O_2$	$SO + SO_3 \rightarrow 2SO_2$	1
R*39	$S^*O + HCO \rightarrow HS^*O + OC$	$SO + HCO \rightarrow HSO + OC$	1
R*40	$H + S^*O + M \rightarrow HS^*O + M$	$H + SO + M \rightarrow HSO + M$	1
R*41	$HS^*O_3 + O_2 \rightarrow HO_2 + S^*O_3$	$HSO_3 + O_2 \rightarrow HO_2 + SO_3$	1
R*42	$HS^*O_3 + OH \rightarrow H_2O + S^*O_3$	$HSO_3 + OH \rightarrow H_2O + SO_3$	1
R*43	$HS^*O_3 + H \rightarrow H_2 + S^*O_3$	$HSO_3 + H \rightarrow H_2 + SO_3$	1
R*44	$HS^*O_3 + O \rightarrow OH + S^*O_3$	$HSO_3 + O \rightarrow OH + SO_3$	1
R*45	$S^*O_3 + H_2O \rightarrow H_2S^*O_4$	$SO_3 + H_2O \rightarrow H_2SO_4$	1
R*46	$H_2S^* + OH \rightarrow H_2O + HS^*$	$H_2S + OH \rightarrow H_2O + HS$	1
R*47	$H_2S^* + H \rightarrow H_2 + HS^*$	$H_2S + H \rightarrow H_2 + HS$	1
R*48	$H_2S^* + O \rightarrow OH + HS^*$	$H_2S + O \rightarrow OH + HS$	1
R*49	$HS^* + O \rightarrow H + S^*O$	$HS + O \rightarrow H + SO$	1
R*50	$HS^* + O_2 \rightarrow OH + S^*O$	$HS + O_2 \rightarrow OH + SO$	1
R*51	$HS^* + HO_2 \rightarrow H_2S^* + O_2$	$HS + HO_2 \rightarrow H_2S + O_2$	1
R*52	$HS^* + HS \rightarrow H_2S^* + S$	$HS + HS \rightarrow H_2S + S$	1
R*53	$HS^* + HS \rightarrow H_2S + S^*$	$HS + HS \rightarrow H_2S + S$	1
R*54	$HS^* + HCO \rightarrow H_2S^* + CO$	$HS + HCO \rightarrow H_2S + CO$	1
R*55	$HS^* + H \rightarrow H_2 + S^*$	$HS + H \rightarrow H_2 + S$	1
R*56	$HS^* + S \rightarrow H + S^*S$	$HS + S \rightarrow H + S_2$	1
R*57	$HS + S^* \rightarrow H + S^*S$	$HS + S \rightarrow H + S_2$	1
R*58	$HS^* + O_3 \rightarrow HS^*O + O_2$	$HS + O_3 \rightarrow HSO + O_2$	1

R*59	$HS^* + NO_2 \rightarrow HS^*O + NO$	$HS + NO_2 \rightarrow HSO + NO$	1
R*60	$HS^* + H_2CO \rightarrow H_2S^* + HCO$	$HS + H_2CO \rightarrow H_2S + HCO$	1
R*61	$S^* + O_2 \rightarrow S^*O + O$	$S + O_2 \rightarrow SO + O$	1
R*62	$S^* + OH \rightarrow S^*O + H$	$S + OH \rightarrow SO + H$	1
R*63	$S^* + HCO \rightarrow HS^* + CO$	$S + HCO \rightarrow HS + CO$	1
R*64	$S^* + HO_2 \rightarrow HS^* + O_2$	$S + HO_2 \rightarrow HS + O_2$	1
R*65	$S^* + HO_2 \rightarrow S^*O + OH$	$S + HO_2 \rightarrow SO + OH$	1
R*66	$S^* + O_3 \rightarrow S^*O + O_2$	$S + O_3 \rightarrow SO + O_2$	1
R*67	$S^* + CO_2 \rightarrow S^*O + CO$	$S + CO_2 \rightarrow SO + CO$	1
R*68	$S^* + S + M \rightarrow S^*S + M$	$S + S + M \rightarrow S_2 + M$	2
R*69	$S^* + S_2 + M \rightarrow S^*S_2 + M$	$S + S_2 + M \rightarrow S_3 + M$	1
R*70	$S^* + S^*S + M \rightarrow S^*S_2 + M$	$S + S_2 + M \rightarrow S_3 + M$	1
R*71	$S^* + S_3 + M \rightarrow S^*S_3 + M$	$S + S_3 + M \rightarrow S_4 + M$	1
R*72	$S^* + S^*S_2 + M \rightarrow S^*S_3 + M$	$S + S_3 + M \rightarrow S_4 + M$	1
R*73	$S^*S + O \rightarrow S^* + SO$	$S_2 + O \rightarrow S + SO$	0.5
R*74	$S^*S + O \rightarrow S + S^*O$	$S_2 + O \rightarrow S + SO$	0.5
R*75	$S^*S + S_2 + M \rightarrow S^*S_3 + M$	$S_2 + S_2 + M \rightarrow S_4 + M$	2
R*76	$S^*S_3 + S_4 + M \rightarrow S^*S_7(AER) + M$	$S_4 + S_4 + M \rightarrow S_8(AER) + M$	2
R*77	$HS^*O + NO \rightarrow HNO + S^*O$	$HSO + NO \rightarrow HNO + SO$	1
R*78	$HS^*O + OH \rightarrow H_2O + S^*O$	$HSO + OH \rightarrow H_2O + SO$	1
R*79	$HS^*O + H \rightarrow HS^* + OH$	$HSO + H \rightarrow HS + OH$	1
R*80	$HS^*O + H \rightarrow H_2 + S^*O$	$HSO + H \rightarrow H_2 + SO$	1
R*81	$HS^*O + HS \rightarrow H_2S + S^*O$	$HSO + HS \rightarrow H_2S + SO$	1
R*82	$HSO + HS^* \rightarrow H_2S^* + SO$	$HSO + HS \rightarrow H_2S + SO$	1
R*83	$HS^*O + O \rightarrow OH + S^*O$	$HSO + O \rightarrow OH + SO$	1
R*84	$HS^*O + S \rightarrow HS + S^*O$	$HSO + S \rightarrow HS + SO$	1
R*85	$HSO + S^* \rightarrow HS^* + SO$	$HSO + S \rightarrow HS + SO$	1

2. We have added all the sulfur chemistry from the Archean code except for reactions involving sulfur polymers ($S_2, S_3, S_4, \ldots$). We demonstrate in Results that S_2 is not formed in significant quantities in high-O_2 atmospheres; hence, higher-sulfur polymers can be safely neglected.
3. We have included production, growth, and deposition of sulfate aerosols, as in the Archean code.

The numerical procedure remained similar to the Archean code.

RESULTS

MIF in the Archean atmosphere

In our calculations of a mildly reducing Archean atmosphere we assumed that reduced gases dominate, as they must have in order to be consistent with evidence from the geologic record. We assumed that photosynthetic production of oxygen was negligible except in localized "oxygen" oases, which were limited to regions of high productivity in the oceans (see Discussion). The only abiotic source of oxygen, photolysis of CO_2, produces surface oxygen mixing ratios of only $\sim 10^{-14}$ PAL (Kasting, 1993; Pavlov *et al.*, 2001).

We kept the surface methane flux fixed at 1.9×10^{11} molecules cm^{-2} s^{-1}. This flux reproduces the present-day CH_4 mixing ratio of 1.6 ppm in our high-O_2 photochemical model. A more accurate calculation with a two-dimensional model by Houghton *et al.* (1994) produces the modern methane flux value of 535 Tg(CH_4)/year (1.2×10^{11} molecules cm^{-2} s^{-1}), a value 30% smaller than ours. This points out the limitation of the one-dimensional modeling approach. It is worth noting that the same surface methane flux (1.9×10^{11} molecules cm^{-2} s^{-1}) used in our oxygen-free Archean atmosphere model resulted in a methane mixing ratio of ~820 ppm as a result of the reduced concentrations of OH and O radicals and the correspondingly longer lifetime of CH_4. Surface boundary conditions for the other atmospheric species were kept the same as in Pavlov *et al.* (2001).

We first performed a set of numerical experiments in an attempt to reproduce the experimental data of Farquhar *et al.* (2001) on sulfur isotopes in sedimentary sulfides and sulfates from 3.3 to 3.5 Ga. Farquhar *et al.* (2001) tried to link MIF in Archean sediments with MIF of sulfur

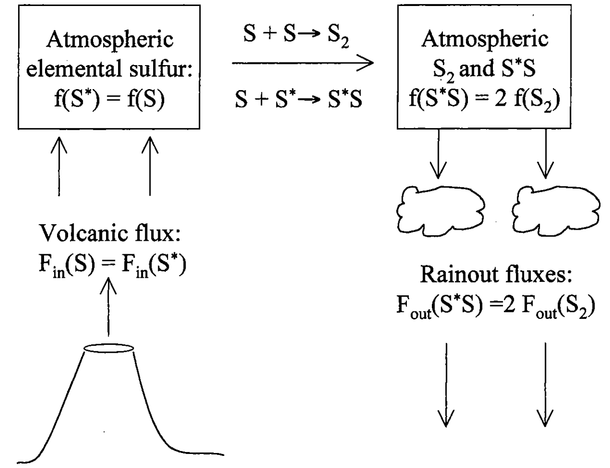

FIG. 1. Schematic diagram of the major (S) and minor (S*) sulfur isotope species budget in the atmosphere (see text).

during SO_2 photolysis. Our photochemical model allowed us to track how the MIF signature from SO_2 photolysis would propagate into different sulfur-bearing species, which in turn would be deposited on the surface and eventually become incorporated in sediments. Not enough laboratory measurements of isotopic fractionation during SO_2 photolysis have been made to do a definitive study. For example, Farquhar *et al.* (2000b, 2001) studied MIF during the photolysis of SO_2 by measuring the isotopic composition of the product elemental sulfur and the residual SO_2. However, SO and probably HS and HSO should also be formed in this experiment, but their isotopic compositions are unknown. Therefore, we can only make some preliminary guesses as to what types of isotopic separation must occur in order to produce the observed fractionation pattern. We argue later that our basic conclusions regarding Archean atmospheric O_2 concentrations are independent of the details of the isotopic fractionation process.

Farquhar's data can be replotted on a diagram that shows the relative ^{33}S and ^{34}S abundances of sedimentary sulfides and sulfates (Fig. 2). The sulfides lie above and to the left of the mass-dependent fractionation line (MFL); the sulfates lie below and to the right. In the more recent experiments on SO_2 photolysis (Farquhar *et al.*, 2001), the degree of fractionation of sulfur isotopes is a function of the length of time during which the gas mixture was exposed to UV radiation. The actual fractionation during photolysis is unknown. Therefore, we simply assumed an arbitrary fractionation in ^{34}S ($\delta^{34}S = -10‰$) and then predicted the relative abundance of ^{33}S using Farquhar's empirical MIF relationship, $\delta^{33}S \approx 0.649\delta^{34}S$.

The fractionation of sulfur isotopes in our photochemical model was implemented by adjusting the relative photolysis rates of $^{33}SO_2$ and $^{34}SO_2$. If "*J*" represents the photolysis rate, then $\delta^{34}S = -10\%$ required that $J(^{34}SO_2) = 0.99J(^{32}SO_2)$ and $J(^{33}SO_2) = 0.99351J(^{32}SO_2)$. Figure 3 displays the isotopic composition of the atmospheric sulfur-bearing species when these rates are used in the model. The resulting isotopic distribution, which moved away from the normal MFL, bears no resemblance to the pattern exhibited by the data in Fig. 2. If, however, we changed the photolysis rates of $^{33}SO_2$ and $^{34}SO_2$ relative to $^{32}SO_2$ so that $J(^{34}SO_2) = 0.99J(^{32}SO_2)$ and $J(^{33}SO_2) = 1.01J(^{32}SO_2)$, we could produce a fractionation pattern that moved in the right direction (Fig. 4). The photolysis products still fall along a straight line, though, which is not what was observed with the data.

As pointed out by Farquhar *et al.* (2001), to produce the observed nonlinear distribution one needs to invoke two or more separate, MIF processes (Fig. 5). In multiphoton photolysis experiments at 248 nm (Wilson *et al.*, 1982), SO_2 is known to photolyze along an additional branch:

$$SO_2 + h\nu \rightarrow S + O_2$$

If the isotopic separation in this branch is different from that in the branch leading to SO + O, a pattern that is roughly similar to that seen in the data can be produced. Recall that these are only preliminary experiments, however, because neither the branching ratio for this reaction nor the actual isotopic fractionation is well known. Furthermore, there is no *a priori* reason why atmospheric H_2S, HS, S, and HSO should end up in sedimentary sulfides and atmospheric SO_2 and H_2SO_4 end up in sulfate minerals. Nonatmospheric chemical processes (e.g., biological sulfate reduction) may further scramble the isotopic signal before it is preserved.

Despite all of these uncertainties, useful information can still be obtained from our model. The MIF produced by atmospheric photochemistry would not be preserved if the products were all rehomogenized in the ocean in the form of dissolved sulfate, which is what would happen today if SO_2 was photolyzed at high altitudes. The only way to preserve MIF is for the photolysis products to leave the atmosphere in different

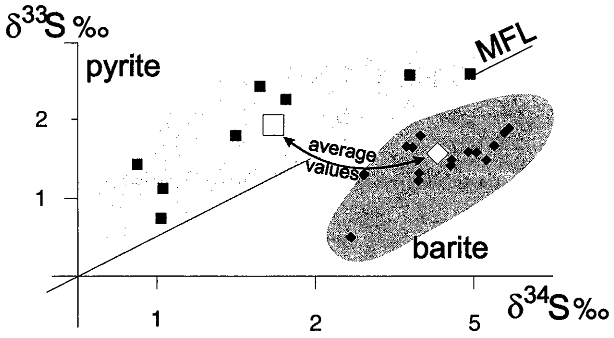

FIG. 2. Data from 3.3–3.5 Ga sedimentary sulfides and sulfates. [Data from Farquhar *et al.* (2000b); figure reproduced by permission of American Geophysical Union from Farquhar *et al.* (2001).] All Phanerozoic sulfides and sulfates plot along the MFL line.

chemical forms. Figure 6 shows the removal rates of the various sulfur-containing species in our model Archean atmosphere. Sulfur species are removed by a combination of wet and dry deposition, as described in the Appendix (see also Kasting, 1990). At least five different species are quantitatively important. Note that the deposition fluxes of H_2S and SO_2 are of the same order of magnitude in the Archean atmosphere (Fig. 6). Therefore, atmospheric MIF in sulfur isotopes could have been preserved after deposition of both reduced and oxidized sulfur-bearing species. This is the key to explaining the data of Farquhar *et al.* (2001).

MIF in higher-O_2 atmospheres

The simulations described above show that it is possible, in principle, to produce a mass-independent S isotope signature in a low-O_2 "Archean" atmosphere. We now demonstrate that the converse of this statement is also true: It is *not* possible to produce a mass-independent isotopic signature in a high-O_2 atmosphere. Indeed, even if we reduce the atmospheric O_2 concentration to 10^{-5} PAL, it still appears unlikely that any type of mass-independent sulfur isotopic signature can be preserved. Thus, we can use the data of Farquhar *et al.* (2001) to place an upper bound on the abundance of O_2 in the Archean atmosphere.

To show this, we performed a set of calculations starting from the present-day atmosphere and progressively decreased the amount of O_2 down to 10^{-5} PAL. First, we fixed the mixing ratios of the atmospheric trace gases H_2, CH_4, CO, N_2O, and CH_3Cl at their present values (at 1 PAL of O_2) and used the photochemical model to calculate their surface fluxes. Those fluxes were -6.8×10^9, 1.96×10^{11}, 2.9×10^{11}, 1.07×10^9, and 5.5×10^8 molecules $cm^{-2}\ s^{-1}$ for H_2, CH_4, CO, N_2O, and CH_3Cl, respectively (minus means the flux is downward). We then kept those fluxes fixed for all low-O_2 simulations. Though this assumption may not be correct without explicitly modeling the biological sources of these gases, it is reasonable.

Note that a decrease in O_2 concentrations below that in the modern atmosphere does not necessarily imply an increase in the concentrations of reduced gases. Figure 7 shows CH_4, CO, and H_2 abundances under reduced oxygen conditions. All three gases are slightly more abundant at 0.1 PAL of O_2. However, below this O_2 level, their concentrations decrease dramatically. At these low O_2 levels, water vapor can be photolyzed in the troposphere, leading to greatly increased OH abundances, and thus shorter photochemical lifetimes for reduced gases (Kasting and Donahue, 1980). Atmospheres with "intermediate" O_2 concentrations (10^{-5}–10^{-2} PAL) are very oxidizing.

Figure 8a demonstrates that at O_2 concentrations $>10^{-5}$ PAL the dominant sulfur-bearing species lost to the ocean are SO_2 and H_2SO_4 (sulfate aerosols). By contrast, in a reducing Archean atmosphere, the removal rates of H_2S and S_8 are comparable to, or even exceed, that of SO_2 (Fig. 6). We did not include higher-sulfur polymers (S_2, S_3, . . . and S_8) in our high-O_2 atmosphere calculations.

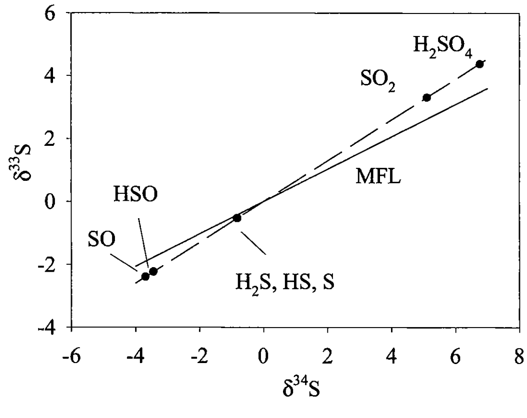

FIG. 3. Model-derived sulfur isotopic composition based on laboratory experiments by Farquhar *et al.* (2000b). We applied the measured isotopic fractionation to the reaction:

$$SO_2 + h\nu \rightarrow SO + O$$

The photolysis rates, $J(SO_2)$, were assumed to obey:

$$J(^{34}SO_2) = 0.99J(^{32}SO_2);\ J(^{33}SO_2) = 0.99351J(^{32}SO_2)$$

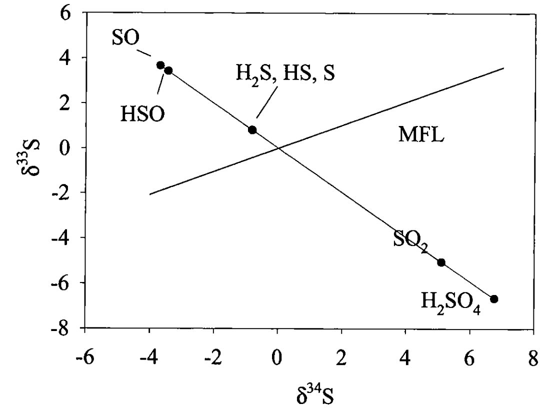

FIG. 4. A model calculation similar to that in Fig. 3, but with

$$J(^{34}SO_2) = 0.99J(^{32}SO_2);\ J(^{33}SO_2) = 1.01J(^{32}SO_2)$$

The relative fractionation between ^{33}S and ^{34}S is arbitrary, but it does produce an isotope diagram with sulfides and sulfates on the correct sides of the MFL.

However, Fig. 8b shows that the production rate of S_2 molecules in our mildly reducing Archean atmosphere is $>10^8$ times higher than in the high-O_2 atmospheres. Therefore, the abundance of S_8 aerosols and other reduced sulfur polymers should be totally negligible in high-O_2 atmospheres.

DISCUSSION

Uncertainties in the calculations

Our atmospheric models are simplified in that they contain no explicit treatment of aqueous-phase redox chemistry in cloud droplets. Therefore, our deposition fluxes of SO_2 and H_2SO_4 aerosols are not entirely correct. In the present atmosphere, ~30% of SO_2 emissions make it back to the surface as SO_2 (Galloway and Whelpdale, 1980). Also, globally today, ~40% of SO_2 oxidation to H_2SO_4 occurs in the gas phase and ~60% in the raindrop (Karamchandani and Venkatram, 1992; McHenry and Dennis, 1994). Most of the SO_2 oxidation in the liquid phase in raindrops occurs by way of reaction with hydrogen peroxide: $SO_2 + H_2O_2 \rightarrow H_2SO_4$. This process should have been important at lower O_2 levels as well. Kasting *et al.* (1985) have demonstrated that tropospheric H_2O_2 abundances decrease only slightly with decreasing O_2 down to 10^{-5} PAL of O_2. Above 10^{-3} PAL of O_2, its concentration in rainwater remains essentially constant (Fig. 9). Thus, the addition of explicit aqueous SO_2 oxidation chemistry to our model should affect the relative deposition fluxes of SO_2 (making it smaller) and H_2SO_4 aerosols (making it higher) in our high-O_2 atmospheres (Fig. 8a). None of this should affect our overall conclusions, however, because after deposition from a high-O_2 atmosphere, SO_2 is likely to be subsequently oxidized to H_2SO_4 in the ocean. It will thus be rehomogenized isotopically, losing any signature of MIF.

Neglecting aqueous SO_2 oxidation chemistry in our reducing Archean atmosphere has even less of an impact on our conclusions. Figure 9 demonstrates that the amount of the major oxidant in the liquid phase, H_2O_2, drops dramatically in an oxygen-free atmosphere, while the abundance of the major reducer, H_2CO, increases by an order of magnitude. Hence, while the addition of rainwater redox chemistry would make our model more technically realistic, we do not expect it to alter any of our basic conclusions. In high-O_2 atmospheres ($Po_2 > 10^{-5}$ PAL), all sulfur gases would eventually end up in the ocean as sulfate. In low-O_2 atmospheres ($PO_2 \sim 10^{-14}$ PAL), various reduced sulfur species would remain quantitatively important; hence, MIF produced by atmospheric photochemistry could be preserved in sediments.

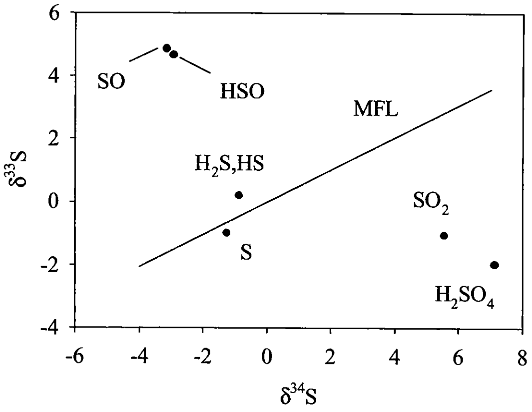

FIG. 5. A model calculation similar to that in Fig. 3, but with an additional branching reaction:

(a) $SO_2 + h\nu \rightarrow SO + O \quad (\times 0.7)$

(b) $SO_2 + h\nu \rightarrow S + O_2 \quad (\times 0.3)$

Branch (a) was assumed to fractionate as in Fig. 4. In branch (b) the fractionation pattern was reversed, i.e.,

$$J(^{34}SO_2) = 1.01J(^{32}SO_2)$$

$$J(^{33}SO_2) = 0.99J(^{32}SO_2)$$

The resulting fractionation pattern (like the data in Fig. 2) does not fall along a single line.

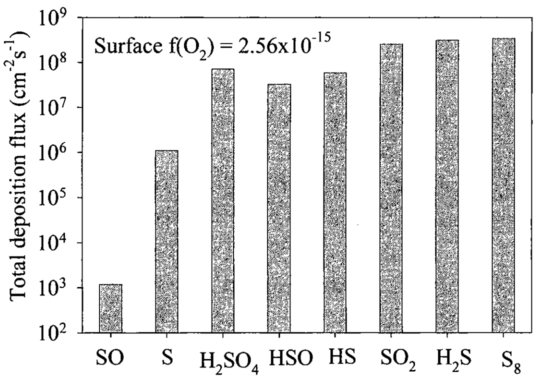

FIG. 6. Combined surface deposition plus rainout fluxes for sulfur species in the mildly reducing Archean model. This assumes no oxygen flux; therefore, the surface mixing ratio $f(O_2)$ is negligible. At least five different sulfur species (in different redox states) are quantitatively significant. This may allow photochemically produced, S isotope MIF to be preserved in sediments.

Oxygen oases

As noted previously, although the majority of the geologic evidence supports low oxygen levels prior to 2.3 Ga, there are strong arguments that photosynthesis was operative as early as 2.7 Ga (Brocks *et al.*, 1999; Summons *et al.*, 1999), at least in some areas of the world's oceans. To simulate such regions of oxygen production we performed a numerical experiment similar to one described by Pavlov *et al.* (2001). We kept the methane mixing ratio fixed at 1,000 ppm (based on balancing volcanic outgassing with escape of hydrogen to space) and performed calculations for different surface "photosynthetic" fluxes of O_2. An increase in the oxygen flux required a corresponding increase in the surface CH_4 flux to maintain a fixed methane mixing ratio. Our results were similar to those reported by Pavlov *et al.* (2001), who showed that the atmospheric O_2 concentration in the vicinity of an oxygen oasis could have been at most 10^{-7} PAL for realistic oxygen and methane production rates and a methane mixing ratio of 1,000 ppm.

An indirect consequence of CH_4 oxidation under high oxygen fluxes in the reducing atmosphere is the high concentration of H_2O_2, which is even more abundant than in the present-day atmosphere. The CH_4 being oxidized creates abundant odd hydrogen (HO_2 and OH) that reacts to form H_2O_2. However, the lifetime of an O_2 molecule in such an atmosphere is at most several hours (Pavlov *et al.*, 2001). For typical wind speeds of ≤50 km/h, this implies that O_2 could spread for at most a few hundred kilometers from its source. Therefore, significant concentrations of O_2 and H_2O_2 should only have existed in limited regions of the troposphere, while the rest of the atmosphere was still almost completely anoxic.

What happens after deposition

An even more important issue that we have not addressed in our calculations concerns the fate of dissolved sulfur species in the Archean ocean. Before these species were removed in sediments, various things could have happened to them. Sulfate, for example, could have been used by bacteria to oxidize organic matter (bacterial sulfate reduction), in which case it may have ended up as pyrite rather than gypsum or barite. Though dissolved SO_2 would not have been oxidized as it is today, it may still have undergone changes in redox state. SO_2 dissociates in solution to form bisulfite (HSO_3^-) and sulfite (SO_3^{-2}). These species are both thermodynamically unstable and are expected to undergo disproportionation reactions to form elemental sulfur, sulfate, and perhaps thiosulfate (S_2O_3) as well. Sulfite and bisulfite may also have been used by bacteria to oxidize organic matter (Skyring and Donnelly, 1982). Thus, the pathways by which MIF in gas-phase sulfur species actually made its way into the sedimentary record remain unknown.

Two basic atmospheric redox states

Not all of the atmospheric O_2 levels shown in our diagrams (Figs. 7–9) are likely to have been

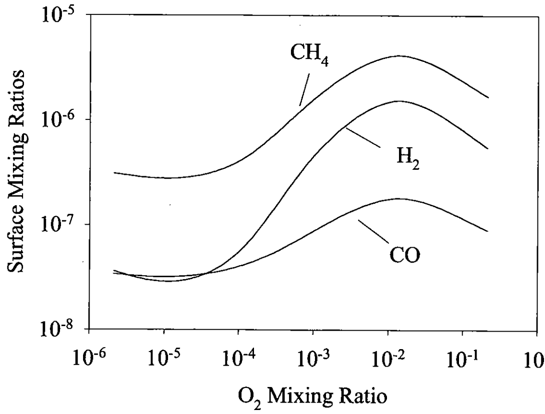

FIG. 7. CH_4, H_2, and CO abundances in oxygen-rich atmospheres. In each calculation, the O_2 concentration and the fluxes of reduced gases (CH_4, H_2, . . .) were kept at fixed values. Note that the decrease in O_2 abundance does not automatically imply an increase in reduced gas concentrations.

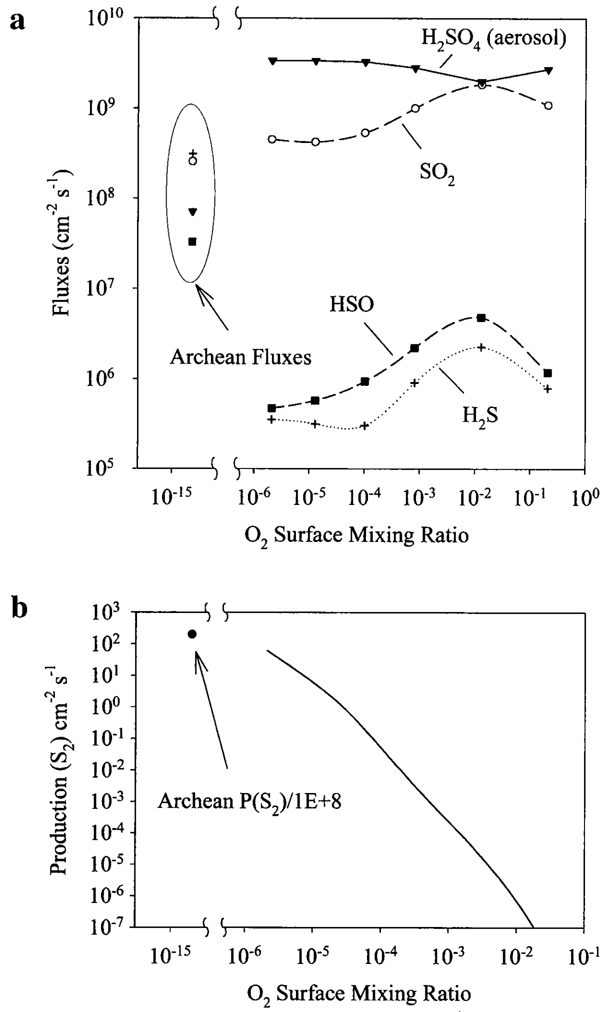

FIG. 8. a: Deposition fluxes of sulfur-bearing species in oxidizing atmospheres (calculations similar to Fig. 7). Over the entire range of O_2 concentrations the dominant deposited sulfur species are SO_2 and H_2SO_4 (both relatively oxidized). Archean fluxes are given for comparison. Here, reduced and oxidized deposition fluxes are comparable (H_2S flux $\approx$ SO_2 flux). **b:** Production rate of S_2 as a function of atmospheric O_2 in oxidizing atmospheres. Although the production rate of S_2 increases with decreasing O_2, its value is still more than eight orders of magnitude less than the production rate of S_2 in the mildly reducing Archean atmosphere. S_2 is the major building block of the higher sulfur polymers S_3, S_4, . . . S_8. Therefore, it is safe to neglect them in oxidizing atmospheres.

physically realized. The initial rise in O_2 around 2.3 Ga almost certainly marked the time at which the net production of O_2 from photosynthesis, followed by organic carbon burial, overwhelmed the volcanic flux of reduced gases (Walker, 1977; Walker *et al.*, 1983; Kasting, 1987; Catling *et al.*, 2001). Once this transition occurred, the atmospheric redox budget would have remained unbalanced until O_2 levels rose high enough to cause efficient oxidative weathering of the continents. It is difficult to determine precisely when this would have happened, but studies of uraninite dissolution and paleosols (Holland, 1984, 1994) suggest that O_2 concentrations of $\geq 10^{-2}$ PAL are required. Hence, atmospheric O_2 probably remained at "Archean" levels ($\leq 10^{-13}$ PAL) for >2 billion years, then rose almost instantaneously from a geologic standpoint to $>10^{-2}$ PAL sometime around 2.3 Ga. Our simulations for O_2 levels between 10^{-5} and 10^{-2} PAL may therefore be relevant to only a very brief period of Earth history.

CONCLUSIONS

The calculations described here provide strong support for the hypothesis that atmospheric O_2 levels increased dramatically around 2.3 Ga. More than that, if our interpretation of the sulfur isotope data is correct, the pre-2.3 Ga atmosphere had to have been essentially anoxic. Our modeling results suggest that atmospheres with as little as 10^{-5} PAL of O_2 would *not* have produced the observed fractionation. Atmospheric MIF would be lost because of the oxidation of sulfur-bearing species to H_2SO_4 and subsequent rehomogenization of the sulfur isotopes. On the other hand, atmospheric MIF in sulfur isotopes can be preserved and recorded in sediments under weakly reduced Archean atmospheric conditions.

Further laboratory work on isotopic fractionation during SO_2 photolysis is obviously needed.

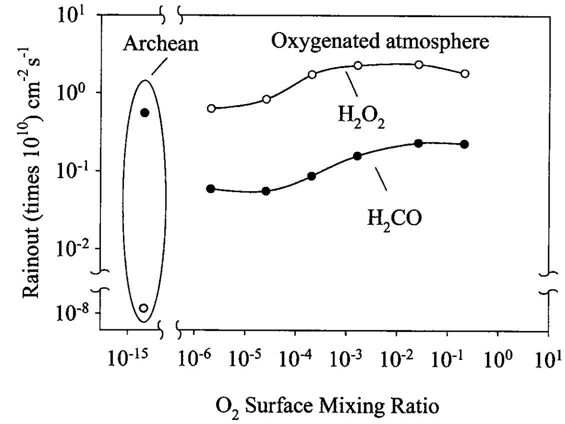

FIG. 9. Rainout rate of oxidants (H_2O_2) and reductants (H_2CO) in the reducing Archean and modern oxidizing atmospheres.

It is not known whether other photochemical processes (e.g., photolysis of H_2S or SO) might be important. The question of how different sulfur species make it from the atmosphere, through the ocean, and into sediments also requires additional study. These research areas should provide fruitful collaborations among laboratory photochemists, biogeochemists, and modelers for some time to come.

APPENDIX: RAINOUT AND SURFACE DEPOSITION OF SULFUR SPECIES

Sulfur species are removed from the photochemical model by a combination of rainout and surface deposition. This appendix describes how these processes are parameterized.

Rainout rates

In our model we used the rainout parameterization of Giorgi and Chameides (1985). Their formulation accounts for the fact that less soluble gases should be removed more slowly than highly soluble ones. This difference is important in our model because the various sulfur gases exhibit a wide range of solubilities. The Giorgi and Chameides (1985) formulation contains a parameter T_W, which represents the average duration of the wet period of the storm cycle (i.e., the length of time that it rains). We took T_W to be 0.5 days, independent of height. For the same values of the function $f(z)$ shown in their Fig. 4, this corresponds to a 5-day complete storm cycle and, hence, a 5-day lifetime for highly soluble species near ground level.

The solubility that enters into the parameterization of Giorgi and Chameides (1985) is not the physical solubility, but rather the "effective" solubility, which takes into account chemical reactions of the dissolved gas within raindrops. SO_2, for example, dissociates in solution to form bisulfite and sulfite ions:

$$(SO_2)_g \leftrightarrow (SO_2)_{aq}$$

$$(SO_2)_{aq} + H_2O \leftrightarrow HSO_3^- + H^+$$

$$HSO_3^- \leftrightarrow SO_3^{2-} + H^+$$

Bisulfite then complexes with methylene glycol (the hydrated form of formaldehyde) according to the following reactions:

$$(H_2CO)_g + H_2O \leftrightarrow CH_2(OH)_2$$

$$CH_2(OH)_2 + HSO_3^- \leftrightarrow H_2O + CH_2OHSO_3^-$$

The effective solubility $H_{eff}(SO_2)$ is related to the physical solubility $H(SO_2)$ by

$$H_{eff}(SO_2)/H(SO_2) = ([SO_2]_{aq} + [HSO_3^-] + [SO_3^{2-}] + [CH_2OHSO_3^-])/[(SO_2)_{aq}]$$

For our low-O_2, Archean model, the total enhancement in SO_2 solubility from these aqueous-phase reactions is $\sim 10^4$.

The equilibria listed above are pH-dependent; hence, it is necessary to include other aqueous-phase reactions that might influence rainfall pH. The most important of these involve CO_2, which hydrates and dissociates in the same manner as SO_2. Sulfuric acid (which dissociates fully in solution) is also important if one considers atmospheres with high sulfur levels. In our model we accounted for dissociation reactions by solving a system of 10 algebraic equations at each time step and at each tropospheric grid point. The relevant equilibrium constants were taken from Chameides (1984). Knowing pH, we can find H_{eff} for all gases. All particles were assumed to rain out at the same rate as the most highly soluble gases.

Surface deposition of gases and particles

The rate at which soluble gases are taken up by the ocean surface was parameterized by assuming an effective deposition velocity (v_{dep}) for each gas. The inverse of this quantity represents the resistance to transfer from the atmosphere to the ocean and may be written as the sum of two terms (Liss, 1971; Slinn *et al.*, 1978; Lee and Schwartz, 1981):

$$\frac{1}{v_{dep}} = \frac{1}{k_g} + \frac{1}{\alpha k_l HRT}$$

The first term on the right represents the atmospheric resistance; k_g is the effective gas-phase mass transfer coefficient, which we take to be 1 cm s^{-1}, following Slinn *et al.* (1978).

The second term on the right in the equation above represents the resistance of the surface layer of the ocean. Here, k_l ($\sim$20 cm h^{-1}) is the liquid-phase mass transfer coefficient, H is the physical Henry's Law coefficient, R is the gas constant, T is temperature, and α is an enhancement coefficient that is related to the effective solubility of the gas (see previous section). According to Lee and Schwartz (1981), the enhancement coefficient is given by

$$\alpha = \frac{\eta}{1 + (\eta - 1)\tanh(k^{1/2})/k^{1/2}}$$

with

$$k = \frac{\tau_{\mathrm{cd}}}{\tau_{\mathrm{r}}} \frac{\eta}{\eta - 1}$$

Here, $\tau_{\mathrm{cd}} = D_{\mathrm{aq}}/k_1{}^2$ (~0.6 s) is a characteristic time describing the competition between convection and diffusion, D_{aq} (2×10^{-5} cm^2 s^{-1}) is the diffusion coefficient for the gas within the liquid boundary layer, τ_{r} is the time constant for hydration of the dissolved gas, and $\eta = H_{\mathrm{eff}}/H$ is the enhancement in solubility due to solvation reactions.

The deposition velocities of the less soluble sulfur gases are limited by their transfer rates through the liquid boundary layer. SO and H_2S, for example, have deposition velocities of 3×10^{-4} and 0.02 cm s^{-1}, respectively. In contrast, deposition of SO_2, HSO, and H_2SO_4 should be limited by the assumed gas-phase transfer rate, except at very low values of ocean pH (Liss, 1971).

Particles can also be lost by surface deposition, although the rate of turbulent diffusion for particles is much smaller than for gases. For particles in the 0.1–1 μm size range, the turbulent deposition velocity is of the order of 0.01 cm s^{-1} (Slinn *et al.*, 1978; Fig. 9). Their effective deposition velocity is the sum of this value plus the fall velocity at the ground.

ABBREVIATIONS

MFL, mass-dependent fractionation line; MIF, mass-independent fractionation; PAL, present atmospheric level.

REFERENCES

Baulch, D.L., Drysdale, D.D., Duxbury, J., and Grant, S.J. (1976) *Evaluated Kinetic Data for High Temperature Reactions, Vol. 3,* Butterworths, London.

Brocks, J.J., Logan, G.A., Buick, R., and Summons, R.E. (1999) Archean molecular fossils and the early rise of eukaryotes. *Science* 285, 1033–1036.

Catling, D.C., Zahnle, K.J., and McKay, C.P. (2001) Biogenic methane, hydrogen escape, and the irreversible oxidation of early Earth. *Science* 293, 839–843.

Chameides, W.L. (1984) The photochemistry of a remote marine stratiform cloud. *J. Geophys. Res.* 89, 4739–4755.

Cloud, P.E. (1972) A working model of the primitive Earth. *Am. J. Sci.* 272, 537–548.

DeAlemeida, A.A. and Singh, P.D. (1986) Photodissociation lifetimes of $^{32}S_2$ molecule in comets. *Earth Moon Planets* 36, 117–125.

DeMore, W.B., Margitan, J.J., Molina, M.J., Watson, R.T., Golden, D.M., Hampson, R.F., Kurylo, M.J., Howard, C.J., and Ravishankara, A.R. (1985) *Chemical Kinetics and Photochemical Data for Use in Stratospheric Modeling, Evaluation No. 7,* JPL Publication 85-37, Jet Propulsion Laboratory, Pasadena, CA.

DeMore, W.B., Golden, D.M., Hampson, R.F., Howard, C.J., Kurylo, M.J., Molina, M.J., Ravishankara, A.R., and Sander, S.P. (1992) *Chemical Kinetics and Photochemical Data for Use in Stratospheric Modeling, Evaluation No. 10,* JPL Publication 92-20, Jet Propulsion Laboratory, Pasadena, CA.

Farquhar, J., Bao, H., and Thiemans, M. (2000a) Atmospheric influence of Earth's earliest sulfur cycle. *Science* 289, 756–758.

Farquhar, J., Savarino, J., Jackson, T. L., and Thiemens, M.H. (2000b) Evidence of atmospheric sulphur in the martian regolith from sulphur isotopes in meteorites. *Nature* 404, 50–52.

Farquhar, J., Savarino, J., Airieau, S., and Thiemens, M.H. (2001) Observation of wavelength-sensitive mass-independent sulfur isotope effects during SO_2 photolysis: application to the early atmosphere. *J. Geophys. Res. Planets* 106, 32829–32839.

Galloway, J.N. and Whelpdale, D.M. (1980) An atmospheric sulfur budget for eastern North America. *Atmos. Environ.* 14, 409–417.

Giorgi, F. and Chameides, W.L. (1985) The rainout parameterization in a photochemical model. *J. Geophys. Res.* 90, 7872–7880.

Herron, J.T. and Huie, R.E. (1980) Rate constants at 298 K for the reactions $SO + SO + M \rightarrow (SO)_2 + M$ and $SO + (SO)_2 \rightarrow SO_2 + S_2O$. *Chem. Phys. Lett.* 76, 322–324.

Hills, H.A., Cicerone, R.J., Calvert, J.G., and Birks, J.W. (1987) Kinetics of the reaction of S_2 with O, O_2, O_3, N_2O, NO, and NO_2. *J. Phys. Chem.* 91, 1199–1204.

Holland, H.D. (1984) *The Chemical Evolution of the Atmosphere and Oceans,* Princeton University Press, Princeton, NJ.

Holland, H.D. (1994) Early Proterozoic atmospheric change. In *Early Life on Earth,* edited by S. Bengtson, Columbia University Press, New York, pp. 237–244.

Houghton, J.T., Meira Filho, L.G., Bruce, J., Lee, H., Callander, B.A., Haites, E., Harris, N., and Maskell, eds. (1994) *Climate Change, 1994: Radiative Forcing of Climate Change and an Evaluation of the IPCC IS92 Emission Scenarios,* Cambridge University Press, Cambridge.

Karamchandani, P. and Venkatram, A. (1992) The role of non-precipitating clouds in producing ambient sulfate during summer: results from simulations with the acid deposition and oxidant model (ADOM). *Atmos. Environ.* 26A, 1041–1052.

Kasting, J.F. (1987) Theoretical constraints on oxygen and carbon dioxide concentrations in the Precambrian atmosphere. *Precambrian Res.* 34, 205–229.

Kasting, J.F. (1990) Bolide impacts and the oxidation state of carbon in the Earth's early atmosphere. *Orig. Life Evol. Biosph.* 20, 199–231.

Kasting, J.F. (1992) Models relating to Proterozoic atmospheric and oceanic chemistry. In *The Proterozoic Biosphere: A Multidisciplinary Study*, edited by J.W. Schopf and C. Klein, Cambridge University Press, Cambridge, pp. 1185–1187.

Kasting, J.F. (1993) Earth's early atmosphere. *Science* 259, 920–926.

Kasting, J.F. and Donahue, T.M. (1980) The evolution of atmospheric ozone. *J. Geophys. Res.* 85, 3255–3263.

Kasting, J.F., Holland, H.D., and Pinto, J.P. (1985) Oxidant abundances in rainwater and the evolution of atmospheric oxygen. *J. Geophys. Res.* 90, 10497–10510.

Kasting, J.F., Zahnle, K.J., Pinto, J.P., and Young, A.T. (1989) Sulfur, ultraviolet radiation, and the early evolution of life. *Orig. Life Evol. Biosph.* 19, 95–108.

Langford, R.B. and Oldershaw, G.A. (1972) Flash photolysis of H_2S. *J. Chem. Soc. Faraday Trans. I* 68, 1550–1558.

Lee, Y.-N. and Schwartz, S.E. (1981) Evaluation of the rate of uptake of nitrogen dioxide by atmospheric and surface liquid water. *J. Geophys. Res.* 86, 11971–11983.

Liss, P.S. (1971) Exchange of SO_2 between the atmosphere and natural waters. *Nature* 233, 327–329.

McElroy, M.B., Wofsy, S.C., and Sze, N.D. (1980) Photochemical sources for atmospheric H_2S. *Atmos. Environ.* 14, 159–163.

McHenry, J.N. and Dennis, R.L. (1994) The relative importance of oxidation pathways and clouds to atmospheric ambient sulfate production as predicted by the regional acid deposition model. *J. Appl. Meteor.* 33, 890–905.

Mojzsis, S.J., Coath, C.D., Greenwood, J.P., McKeegan, K.D., Harrison, T.M., and Runnegar, B. (2001) Non-mass-dependent sulfur isotopes documented from *in-situ* measurements of Precambrian sedimentary sulfides by multi-collector ion microprobe. 11th Annual V.M. Goldschmidt Conference. Available at: http://www.lpi.usra.edu/meetings/gold2001/pdf.program.pdf.

Ohmoto, H. (1996) Evidence in pre-2.2 Ga paleosols for the early evolution of atmospheric oxygen and terrestrial biota. *Geology* 24, 1135–1138.

Ohmoto, H. (1997) When did the Earth's atmosphere become oxic? *Geochem. News* 93, 13.

Okabe, H. (1971) Fluorescence and predissociation of sulfur dioxide. *J. Am. Chem. Soc.* 93, 7095–7096.

Pavlov, A.A., Kasting, J.F., and Brown L.L. (2001) UV-shielding of NH_3 and O_2 by organic hazes in the Archean atmosphere. *J. Geophys. Res.* 106, 23267–23287.

Skyring, T.W. and Donnelly, T.H. (1982) Precambrian sulfur isotopes and a possible role for sulfite in the evolution of bacterial sulfate reduction. *Precambrian Res.* 17, 41–61.

Slinn, W.G.N., Hasse, L., Hicks, B.B., Hogan, A.W., Lal, D., Liss, P.S., Munnich, K.O., Sehmel, G.A., and Vittori, O. (1978) Some aspects of the transfer of atmospheric trace constituents past the air-sea interface. *Atmos. Environ.* 12, 2055–2087.

Sullivan, J.O. and Holland, A.C. (1966) *NASA Technical Report: A Congeries of Absorption Cross Sections for Wavelengths Less Than 3000 Å*, Publication CR371, NASA, Washington, DC.

Summons, J.R., Jahnke, L.L., Hope, J.M., and Logan, G.A. (1999) 2–Methylhopanoids as biomarkers for cyanobacterial oxygenic photosynthesis. *Nature* 400, 554–557.

Thiemens, M.H. (1999) Atmosphere science—mass-independent isotope effects in planetary atmospheres and the early solar system. *Science* 283, 341–345.

Toon, O.B., McKay, C.P., Ackerman, T.P., and Santhanam, K. (1989) Rapid calculation of radiative heating rates and photodissociation rates in inhomogeneous multiple scattering atmospheres. *J. Geophys. Res.* 94, 16287–16301.

Towe, K.M. (1994) Earth's early atmosphere: constraints and opportunities for early evolution. In *Early Life on Earth*, edited by S. Bengtson, Columbia University Press, New York, pp. 36–47.

Turco, R.P., Hamill, P., Toon, O.B., Whitten, R.C., and Kiang, C.S. (1979) A one-dimensional model describing aerosol formation and evolution in the stratosphere: I. Physical processes and mathematical analogs. *J. Atmos. Sci.* 36, 699–717.

Turco, R.P., Whitten, R.C., and Toon, O.B. (1982) Stratospheric aerosols: observation and theory. *Rev. Geophys.* 20, 233–279.

Walker, J.C.G. (1977) *Evolution of the Atmosphere*, Macmillan, New York.

Walker, J.C.G., Klein, C., Schidlowski, M., Schopf, J.W., Stevenson, D.J., and Walter, M.R. (1983) Environmental evolution of the Archean-Early Proterozoic Earth. In *Earth's Earliest Biosphere: Its Origin and Evolution*, edited by J.W. Schopf, Princeton University Press, Princeton, NJ, pp. 260–290.

Warneck, P., Marmo, F.F., and Sullivan, J.O. (1964) Ultraviolet absorption of SO_2: dissociation energies of SO_2 and SO. *J. Chem. Phys.* 40, 1132–1136.

Wilson, M.W., Rothschild, M., Muller D.F., and Rhodes, C.K. (1982) Multiphoton photofragmentation of SO_2 at 248 nm. *J. Chem. Phys.* 77, 1837–1841.

Yung, Y.L. and DeMore, W.B. (1982) Photochemistry of the stratosphere of Venus: implications for atmospheric evolution. *Icarus* 51, 199–247.

Zmolek P., Xu, X.P., Jackson, T., Thiemens, M.H., and Trogler, W.C. (1999) Large mass independent sulfur isotope fractionations during the photopolymerization of (CS2)-C-12 and (CS2)-C-13. *J. Phys. Chem.* 103, 2477–2480.

Address reprint requests to:
Dr. Alexander A. Pavlov
Laboratory for Atmospheric and Space Physics
University of Colorado
Duane Physics Building, Room D221
392 UCB
Boulder, CO 80309–0392

E-mail: pavlov@lasp.colorado.edu